Nuclear Instruments and Methods in Physics Research A 346 (1994) 168–176
North-Holland

NUCLEAR INSTRUMENTS & METHODS IN PHYSICS RESEARCH
Section A

# Response of TAPS to monochromatic photons with energies between 45 and 790 MeV

A.R. Gabler [a], W. Döring [a], M. Fuchs [a], B. Krusche [a], V. Metag [a], R. Novotny [a,*], M. Röbig-Landau [a], H. Ströher [a], V. Tries [a], C. Molenaar [b], H. Löhner [b], J.H.G. van Pol [b], A. Raschke [b], M. Šumbera [b], L.B. Venema [b], H.W. Wilschut [b], R. Averbeck [c], W. Niebur [c], A. Schubert [c], R.S. Simon [c], R. Beck [d], J. Peise [d], G.J. Miller [e], R.O. Owens [e], G. Anton [f]

[a] *II. Physikalisches Institut, Universität Giessen, D-35392 Giessen, Germany*
[b] *Kernfysisch Versneller Instituut, NL-9747 AA Groningen, The Netherlands*
[c] *Gesellschaft für Schwerionenforschung, D-64220 Darmstadt, Germany*
[d] *Institut für Kernphysik, Universität Mainz, D-55128 Mainz, Germany*
[e] *Department of Physics and Astronomy, University Glasgow, Glasgow G75 0QU, UK*
[f] *Physikalisches Institut, Universität Bonn, D-53115 Bonn, Germany*

(Received 25 February 1994)

The Two Arm Photon Spectrometer TAPS – comprising 384 plastic–$BaF_2$ scintillator telescopes – was tested with monochromatic photons in the energy range between 45 and 790 MeV. The energy resolution for a collimated photon beam hitting the central detector module was determined to $\sigma/E = 0.59\% \times E_\gamma^{-1/2} + 1.9\%$ ($E_\gamma$ given in GeV). For the the fast scintillation component alone $\sigma/E = 0.79\% \times E_\gamma^{-1/2} + 1.8\%$ has been measured. The position resolution of the point of impact amounts to $\Delta x = 2$ cm (FWHM) at the highest energies which corresponds to 30% of the diameter of an individual module. Monte Carlo simulations using the code GEANT3 are in good agreement with the experimental results.

## 1. Introduction

The design of many state-of-the-art spectrometers for high energy photon detection is based on Monte Carlo simulations of the electromagnetic shower as provided by the computer codes EGS4 or GEANT3 [1]. It is thus of great interest to compare the experimental photon response achieved with such predictions. The detector system TAPS was optimized to identify neutral mesons by an invariant mass analysis of the two decay photons. This requires the simultaneous measurement of the point of impact and the energy of the photons and, consequently, relies on a detailed knowledge of the experimental line shape and an appropriate method of position reconstruction.

As part of the experimental program, the photon spectrometer TAPS was installed at the Mainz Microtron (MAMI) to study photonuclear reactions. This allowed a dedicated measurement of the response function to quasi-monochromatic photons in the energy range from $E_\gamma = 45$ to 790 MeV produced by bremsstrahlung tagging.

A brief description of the spectrometer in section 2 is followed by the details of the experimental set-up and the measurements performed (section 3). Section 4 contains the analysis of the data and the discussion of the experimental energy and position resolution in comparison to GEANT3 simulations.

## 2. The two arm photon spectrometer TAPS

TAPS (Two Arm Photon Spectrometer) is a detector array which comprises 384 individual detector telescopes developed by an international collaboration [2]. The instrumental concept has allowed one to perform a very broad spectrum of experiments at different accelerator facilities exploiting the large dynamic range of the detector system (1 MeV to 15 GeV), the modularity of the device and the flexibility in the geometrical arrangement. These measurements include bremsstrahlung and $\pi^0$ production in heavy ion collisions at GANIL, $\pi^0$ and $\eta$ production in relativistic heavy ion collisions, studies of the two-phonon giant resonances in peripheral reactions at GSI, photoproduction of neutral mesons at MAMI, as well as meson Dalitz decays at the CERN SPS.

An individual detector telescope consists of a $BaF_2$-crystal and a separate NE102A plastic scintillator positioned in front as illustrated in Fig. 1. The hexagonally

* Corresponding author. Tel. +49 641 702 2777, fax +49 641 74390, e-mail rainer@piggy.physik.uni-giessen.de.


*SSDI* 0168-9002(94)00353-9

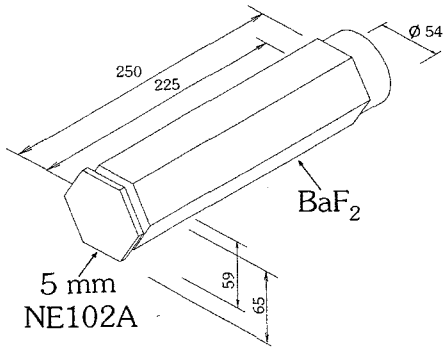


Fig. 1. Geometry of the active parts of an individual module. The dimensions are in mm.

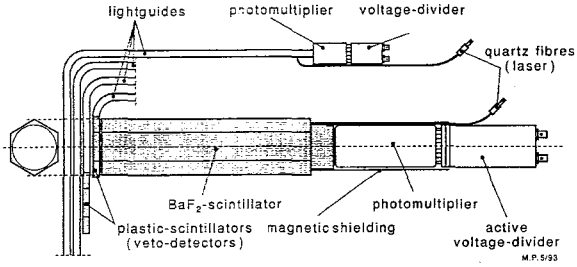


Fig. 2. Assembled NE102A $BaF_2$ detector telescope: The $BaF_2$ module consists of the hexagonal crystal coupled directly to a photomultiplier with silicon grease, the voltage divider, the magnetic shielding and the quartz fiber. In front of the photon detector the four layers of plastic veto counters including the optical readout are indicated.

shaped crystals [#1] (diameter of the inscribed circle is 5.9 cm) have an overall length of 25 cm corresponding to 12 radiation lengths $X_0$ including a cylindrical end part of 5.4 cm diameter. The scintillation light is read out directly via a photomultiplier with a fused silica window [#2]. Fig. 2 shows the fully assembled $BaF_2$ module. Similar detectors are incorporated into the CATS spectrometer of the A2 collaboration at Mainz [3].

The hexagonal plastic scintillator of slightly larger diameter and 0.5 cm thickness ($0.01X_0$) is coupled to a photomultiplier [#3] via a Perspex lightguide and serves as an online charged particle veto. For calibration as well as stability control light from a nitrogen laser [#4] is fed into each detector module by a quartz fiber. Detailed technical information is given in ref. [4].

Fig. 3 illustrates one of the six detector blocks which contain 64 individual telescopes each. The veto detectors are split into two sub-groups. In order to accomplish the individual readout the scintillators are arranged in up to four layers which adds on average $0.025X_0$ of plastic material in front of the $BaF_2$ crystal. The modular design of TAPS allows a very flexible arrangement of the blocks in either a movable tower configuration [4] or with all blocks in a horizontal plane around the target position (see below) as chosen in the present set-up.

## 3. The response measurement

### 3.1. Monochrornatic photons

High energy monochromatic photons (above 100 MeV) are not readily obtainable. The only line source available is due to the capture of negative pions on hydrogen, $\pi^- p \rightarrow$ $\gamma n$, which produces photons of $E_\gamma = 129$ MeV on top of a broad spectrum caused by neutral pion decay following $\pi^- p \rightarrow \pi^0 n$. As an alternative, monoenergetic electrons have been widely used but one has to allow for the difference between electromagnetic showers initiated by electrons and by photons [5]. Nowadays it is possible to obtain quasi-monochromatic photons by means of the tagging-technique using high duty-factor electron accelerators [6]. The most frequently used method exploits the tagging of bremsstrahlung produced by a monochromatic electron beam of known energy hitting a thin radiator. After bremsstrahlung emission the electron momenta are analysed by a magnetic spectrometer, while requiring a time-coincidence with a bremsstrahlung photon. This allows the determination of the corresponding photon energy. In order to keep the rate of accidental coincidences as small as possible, a high duty-factor, preferably a cw machine is required [7].

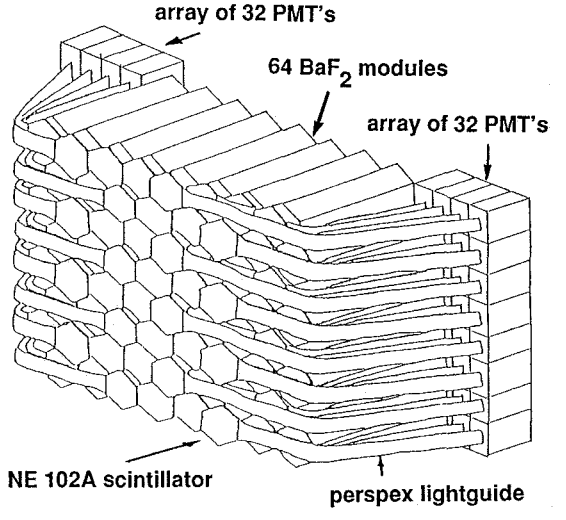


Fig. 3. Assembled TAPS-block consisting of 64 individual plastic/$BaF_2$ detector telescopes.

[#1] Manufactured by Dr. Karl Korth (Kiel, Germany).
[#2] Hamamatsu R2059-01.
[#3] Philips XP2972.
[#4] Laser Scientific Inc., VSL-337.

### 3.2. The experimental set-up at MAMI

The accelerator facility MAMI can provide a cw electron beam up to 855 MeV energy [8]. The quasi-monochromatic photons are tagged using the new Glasgow spectrometer [9] (Fig. 4). The 352 electron detectors in the focal plane can tag photons of energies between 5% and 92% of the incident electron energy and this whole range was used in the present investigation. The energy width per tagging channel varies along the focal plane from $\Delta E = 2.3$ MeV at 45 MeV to $\Delta E = 1.1$ MeV at 790 MeV photon energy, respectively, and has to be accounted for in the data analysis (see below). TAPS was set up at a position approximately 13 m downstream from the bremsstrahlung target as shown schematically in Fig. 4. One block was moved into the direct photon beam which was collimated to a diameter of $d = 1.3$ cm at the front face of the crystal. One central detector of this block was illuminated at various positions (see Fig. 5). Since the selected module was surrounded by a complete number of neighbours and next neighbours, it was possible to sum the entire energy of the electromagnetic shower deposited in the calorimeter.

Fig. 6a illustrates on an arbitrary energy scale the response of TAPS to the total tagged photon spectrum produced by electrons of $E_e = 855$ MeV primary energy. The nearly energy independent tagging efficiency reproduces the typical shape of the full bremsstrahlung spectrum. The upper cut-off corresponds to the maximum tagged photon energy of 790 MeV. Requiring a coincidence with one particular electron channel in the tagger selects a narrow photon energy bin. The spectrum obtained for a chosen mean photon energy of $E_\gamma = 258$ MeV is presented in Fig. 6b.

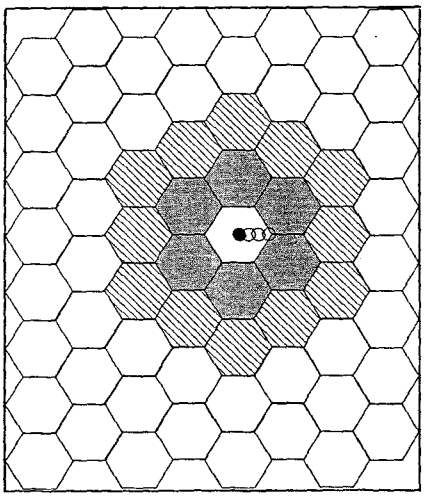

Fig. 5. Position of the illuminated detector within one TAPS-block consisting of 64 $BaF_2$ modules. The full and open circles mark the chosen size and positions of the beam spot.

## 4. Simulations and experimental results

### 4.1. Simulation of the electromagnetic shower

The Monte Carlo code GEANT3 was used to simulate the expected photon response of TAPS. The geometrical

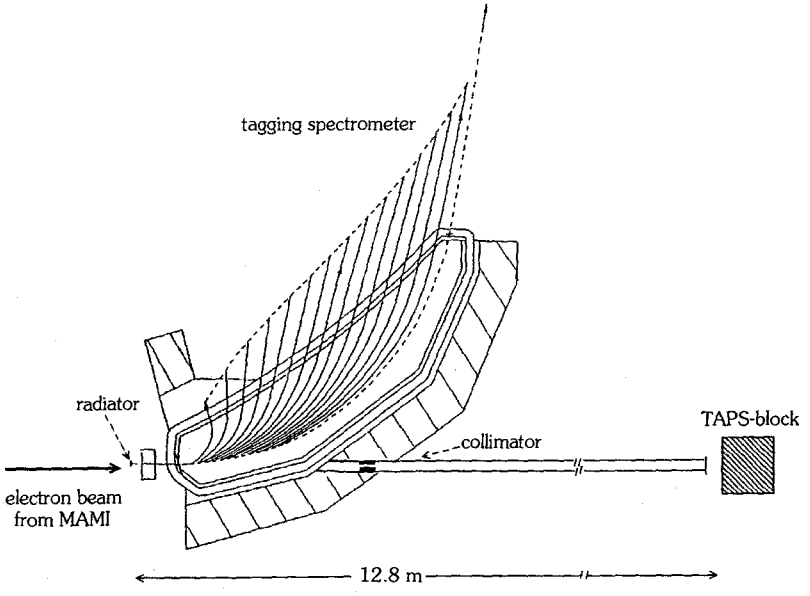


Fig. 4. TAPS set-up at the Mainz Microtron for the response measurement. The bremsstrahlung photons which are produced by the electron beam hitting the radiator are tagged by the momentum analyzed electrons in the Glasgow tagging facility. The collimated photon beam directly hits one TAPS block.

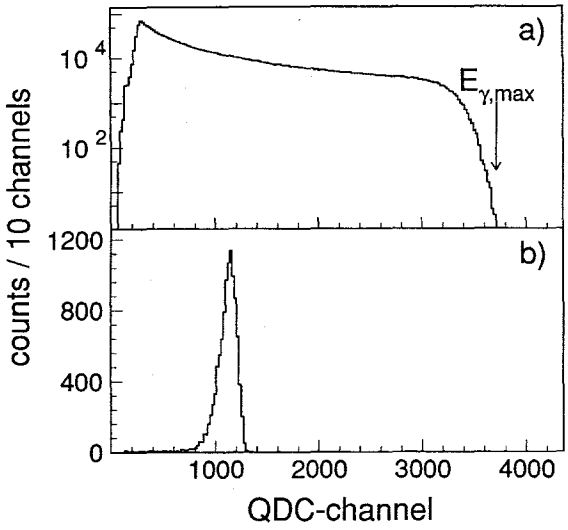


Fig. 6. (a) Response of TAPS to the tagged bremsstrahlung spectrum. $E_{\gamma,max}$ indicates the maximum tagged photon energy. (b) Response of TAPS to tagged photons with energies of $\approx 258$ MeV selected by concidence with the corresponding electrons.

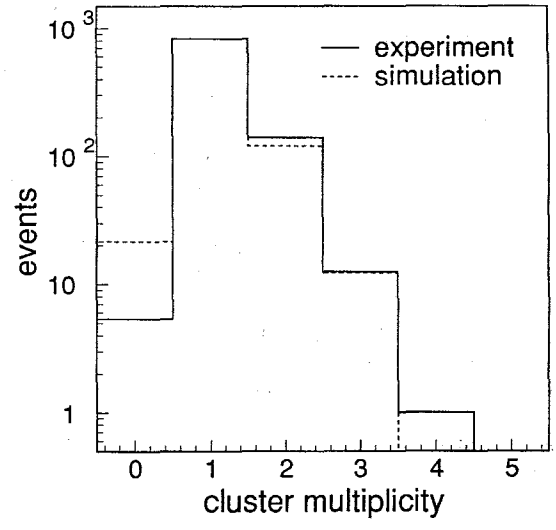


Fig. 7. Multiplicity of identified detector clusters measured at a photon energy of $E_\gamma = 300$ MeV. The dotted histogram represents the GEANT3 simulation.

set-up of one detector array was modelled by the active volume of the 64 $BaF_2$ crystals with a gap of 1 mm between each module filled with plastic to account for the reflector material and detector housing. However, in most of the simulations the material in front due to the plastic veto system has been negelected. An uniform photon beam of 1.3 cm diameter was assumed. Secondary photons and leptons due to the electromagnetic shower are fully tracked down to a kinetic energy of 100 keV.

### 4.2. Shower distributions

The initial interaction of a high energy photon in one detector module will in general trigger several modules due to the lateral distribution of the initiated electromagnetic shower. In reactions where it is known that a single photon has hit a TAPS calorimeter block, it is nearly sufficient to add the signals of just seven detectors, the one with the largest energy deposit and the six surrounding modules, in order to include the complete shower. In the present photon energy range the lateral distribution will be entirely captured when 19 detectors are used (cf. Fig. 5). Because in heavy-ion induced reactions several particles or photons may hit simultaneously one block, such a crude procedure is not applicable since a double hit would nearly always result in overlapping clusters. Therefore, a procedure is required which assigns the individual responding detector clusters to the various incident charged or neutral particles and photons, respectively. A cluster is defined as a group of responding detectors which have to be direct neighbours. Thus the boundary of a cluster is surrounded by non-firing detectors. In addition, all responding detectors should have photon characteristics as determined from time of flight, the absence of a charged particle veto and the appropriate pulse shape of the $BaF_2$ signal as deduced from the integration of the light output over a short and long time gate, respectively. Ideally there would be only one identified cluster per photon impact but this is not always the case. Fig. 7 displays on a logarithmic scale the measured multiplicity of identified clusters for a single tagged photon with energy $E_\gamma = 300$ MeV. In each module a minimum energy deposition of 3 MeV is required corre-

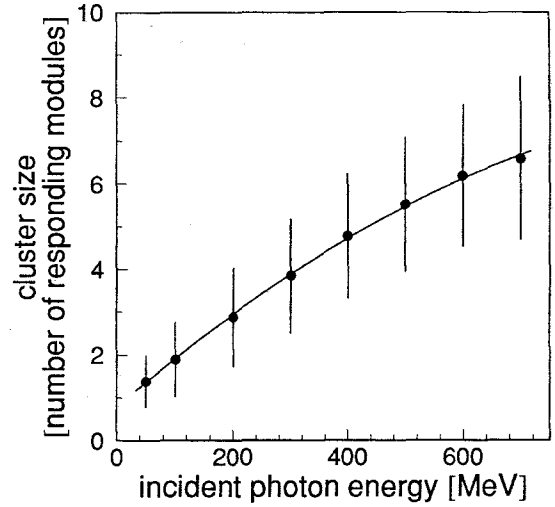


Fig. 8. Measured number of responding detector modules within the identified main cluster shown as a function of the incident photon energy. The bars indicate the width ($\sigma$) of the individual distribution. The energy threshold of each detector was 3 MeV.

sponding to the typical discriminator threshold setting used in most of the TAPS experiments. The probability for at least one additional cluster amounts to $\approx 10\%$ at that particular energy. However, the energy contained in the secondary clusters is generally very small and limited to typically 20 MeV. Photon hits for which no cluster was identified represent rejected events where the particle veto triggered due to charged secondary shower products. Fig. 7 includes the results of GEANT3 simulations analysed under experimental conditions which are in good agreement with the measurement.

Fig. 8 illustrates the measured average clustersize, i.e. the number of responding detector modules in the main cluster, as a function of the incident photon energy. The vertical bars indicate the width ($\sigma$) of the distribution. More details on the cluster distribution can be found in ref. [10].

### 4.3. The energy response

In order to determine the total energy of the electromagnetic shower the signals of all cluster modules which responded must be summed. This requires a relative calibration, which was obtained from the energy loss of cosmic muons detected in each individual $BaF_2$ crystal after correction for the QDC pedestals. The absolute calibration has been obtained from a comparison of the experimental energy response with that predicted by the simulations (see below).

#### 4.3.1. The line shape

The experimental line shape is shown in Fig. 9 for three selected incident photon energies. The two parts of the figure compare the response of the central detector (upper row) to the shape obtained after summing over all modules which responded (lower). The finite incident energy width determined by the chosen tagger channels is given in the labels above the figure. As expected, the shape becomes significantly narrower after adding the lateral leakage of the electromagnetic shower.

A good overall agreement can be achieved in the GEANT3 simulation only if the calculated energy $E_d$, which is deposited into the individual detector module, is folded in addition with a Gaussian of an energy-dependent FWHM, $\Delta E_d/E_d = 3\% \times E_d^{-1/4}$ ($E_d$ given in GeV). This empirical correction accounts for resolution losses in the real detector due to photon statistics, electronic noise and the inefficient collection of the scintillation light which is caused by the reflection losses at the crystal surface and the wavelength-dependent absorption length of the scintillation light within the crystal itself [4]. The latter effects have received full consideration during the development of the detector but are not incorporated into the simulation. The simulated shapes are shown for comparison in Fig. 9.

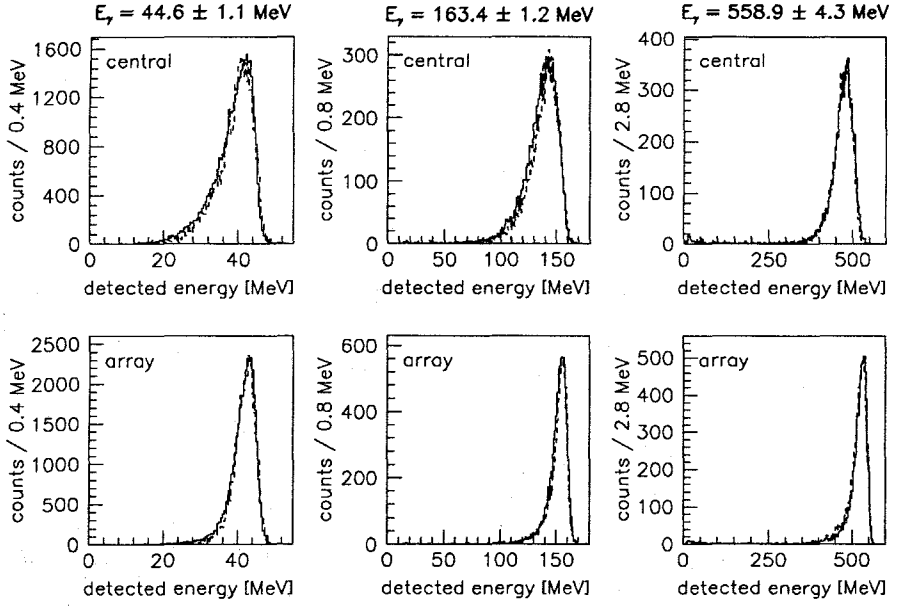


Fig. 9. Comparison of measured TAPS photon response to GEANT3-simulations (dotted line) at three different incident energy bins ($E_\gamma \approx 45$, 163, and 559 MeV). The widths of the energy bins are given in the figure. The line shape is shown for the central module (upper row) and the sum over all detectors which responded (lower row).

The experimental response function has been parametrized by two analytical functions valid below and above the most probable energy $E_{\mathrm{Peak}}$ [11]:

$$y = NG \qquad \text{for } E \geq E_{\mathrm{Peak}},$$

$$y = N\left(G + \exp\left(\frac{E - E_{\mathrm{Peak}}}{\lambda}\right)(1 - G)\right) \qquad \text{for } E \leq E_{\mathrm{Peak}},$$

$$G = \exp\left(-\frac{4 \ln 2 (E - E_{\mathrm{Peak}})^2}{\Gamma^2}\right).$$

The parameter $N$ is used for normalization and the two different width parameters enable the obviously non-Gaussian asymmetric line shape to be reproduced. The FWHM of the Gaussian, $\Gamma$, describes the high energy side of the peak whereas $\lambda$ accounts for the low energy tail. Both parameters appear to be smooth but non-linear functions of the incident photon energy $E_\gamma$ [12], whereas the most probable energy $E_{\mathrm{Peak}}$ is an entirely linear function of the incident photon energy, $E_{\mathrm{Peak}} = 0.962 E_\gamma$. Fig. 10 illustrates the quality of the analytical expression for a photon energy of $E_\gamma = 55$ MeV.

*4.3.2. The energy resolution*

The observed energy resolution $\sigma$ is obtained from the FWHM of the measured line shape $\sigma = \mathrm{FWHM}/2.355$. In order to evaluate the pure detector resolution $\sigma/E_{\mathrm{Peak}}$, the finite incident energy width determined by the tagger granularity has to be unfolded. The values corresponding to zero energy width are extrapolated linearly from the experimental resolutions deduced at different incident energy widths by gating on 1, 2 or 3 adjacent tagger channels.

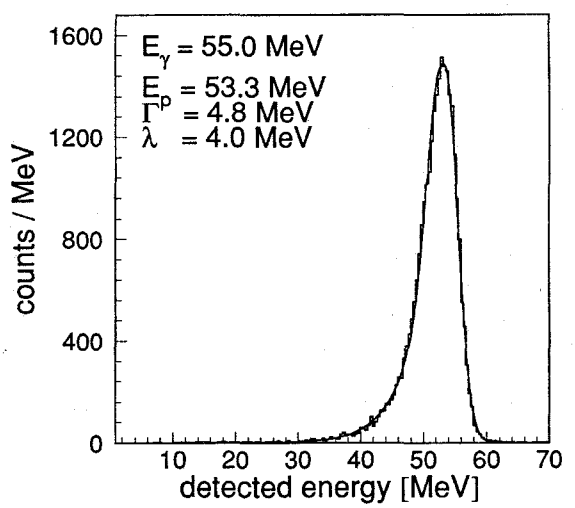


Fig. 10. Experimental line shape measured at $E_\gamma = 55$ MeV compared to the fitted analytical response function. The values of the fit parameters (see text) are shown in the figure.

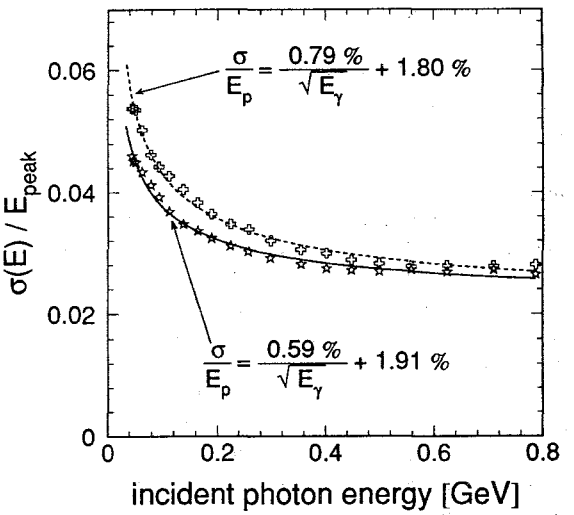


Fig. 11. Measured energy resolution $\sigma/E_{\mathrm{Peak}}$ of the total light output (integration gate 2 $\mu$s), stars, and the fast scintillation component (integration gate 50 ns), crosses, as a function of the incident photon energy. The values are extrapolated to zero incident energy width. The energy dependence has been parametrized by $\sigma/E = \mathrm{A}E^{-1/2} + \mathrm{B}$ as shown in the figure.

It is well known that $BaF_2$ [13] emits two major scintillation components which differ in decay time and scintillation efficiency. The relative intensity of the components is sensitive to the nature of the incident particle. This intrinsic behaviour is exploited by performing a pulse-shape analysis in order to distinguish between photons and charged particles [14]. The intensity of the fast component can be determined in the QDC within a short integration time of typically 50 ns, but the total light output has to be integrated over a gate width of 2 $\mu$s to achieve optimum energy resolution especially at lower energies.

Fig. 11 shows as a function of incident photon energy the energy resolution after extrapolation to zero energy width for a collimated photon beam of 1.3 cm in diameter hitting the center of one detector module. The values are given for the total light output as well as the fast scintillation component alone. The energy dependence has been fitted in both cases with the empirical expression

$$\frac{\sigma(E_\gamma)}{E_{\mathrm{Peak}}} = AE_\gamma^{-1/2} + B,$$

with the energy $E_\gamma$ given in GeV. The results obtained are listed in Table 1 and compared with other detectors.

The resolution value $\sigma/E = 2.50\%$ of the total scintillation output extrapolated to $E_\gamma = 1$ GeV is excellent in comparison to $4\pi$ homogeneous electromagnetic calorimeters such as the Crystal Ball [17], Crystal Barrel [20], Cleo II [19] and L3 [18] facilities. These devices use longer

inorganic crystals (NaI(Tl), CsI(Tl) or BGO scintillators) of 16 and $22X_0$ total crystal length.

As expected, the energy resolutions of both light components become similar at energies above 500 MeV, since the resolution of the fast component, which is less intense by an order of magnitude, is no longer determined by pure photon statistics. Even at lower energies the difference in the resolution is principally due to differences in light collection and optical transparency of the crystal due to the very different emission spectra of the two scintillation components peaking at $\lambda_{fast} = 220$ nm and $\lambda_{slow} = 320$ nm. As a consequence, $BaF_2$ can be used in high resolution calorimetry even at very high count rates by exploiting solarblind photomultipliers, which have a significantly reduced quantum efficiency for photons which originate from the slow scintillation component.

The experimental resolution achieved is compared to GEANT3 simulations in Fig. 12 in which the experimental data are represented as a solid line by the parametrization obtained above. A minimum calculated energy deposition of $E_d = 3$ MeV is required for the individual crystals to be considered in the shower reconstruction. The open crosses show the simulated energy resolution for an ideal detector which is only limited by the energy leakage of the electromagnetic shower due to the limited geometry. The experimental values of the energy resolution can be reproduced (open circles) only by an additional folding of the simulated energy deposition in each module with the Gaussian function of width $\Delta E_d$ described in section 4.3.1.

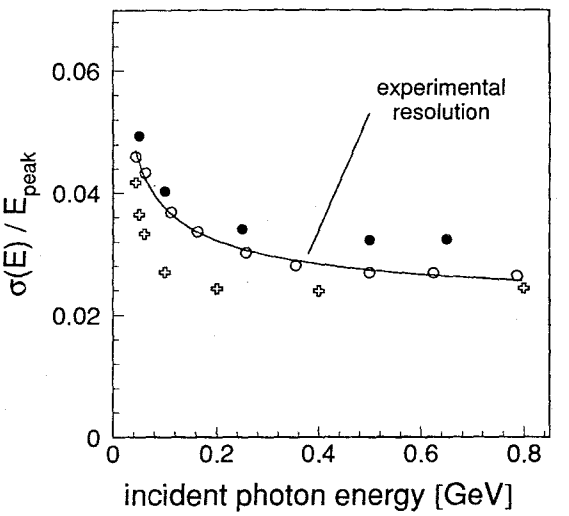


Fig. 12. GEANT3 simulation of the energy resolution. The experimental data for a collimated photon beam impinging at the center of one module are represented by the solid line. The resolution has been simulated under the assumption of shower losses from the active calorimeter volume (open crosses) and also including an additional folding $\Delta_d$ with the energies deposited into the individual detector modules as described in the text (open circles). An energy threshold of 3 MeV is required. The full circles show the effective resolution when the front face of the detector module is fully illuminated.

*4.3.3. Energy response as a function of impact point*

All of the above results have been obtained for central impact of the incident photon beam. However, in an experiment photons illuminate the whole front face of the detector. Therefore, the position dependence of the reconstructed energy response has been investigated by moving the impact point in steps of 1 cm from the center of a single module. Fig. 13 shows the measured line shape for three positions in comparison to central illumination at an energy of $E_\gamma = 257.8$ MeV. The fraction of the energy deposited in the central module decreases drastically when moving the beam spot off center. The resolution of the reconstructed shower energy degrades from $\sigma/E = 3.0\%$ to $\sigma/E = 4.2\%$ and the low energy tail becomes more pronounced. The percentage of the yield $4\sigma$ below the most probable energy $E_{Peak}$ changes from 7% to 17% for photons incident near the junction of three adjacent crystals. The simulation explains these effects which appear to be caused predominantly by the inactive layers between $BaF_2$ crystals. Due to the success achieved in reproducing the individual experimental spectra for collimated photon impact, the energy resolution can be deduced with confidence for a fully illuminated crystal and the experimentally relevant performance can be determined. The results obtained are given in Fig. 12. The influence of the dead material mainly affects higher photon energies due to the increased lateral spread of the electromagnetic shower.

Table 1
Energy resolutions of TAPS measured with tagged photons listed in comparison to the performance of operating homogeneous electromagnetic calorimeters. The table shows the energy resolution given at 1 GeV, the used scintillator material and the length of an individual detector module given in units of radiation length $X_0$

| | $A$ [%] | $B$ [%] | $\sigma(E)/E$ at 1 GeV [%] | Material | $X_0$ |
|---|---|---|---|---|---|
| Fast component (coll. beam) | 0.79 | 1.80 | 2.59 | $BaF_2$ | 12 |
| Total light (coll. beam) | 0.59 | 1.91 | 2.50 | $BaF_2$ | 12 |
| Total light (full illumination) | 0.54 | 2.40 | 2.94 | $BaF_2$ | 12 |
| Crystal Ball [17] | | | 2.70 | NaI(Tl) | 16 |
| Crystal Barrel [20] | | | 2.00 | CsI(Tl) | 16 |
| CLEO II [19] | | | 2.20 | CsI(Tl) | 16 |
| L3 [18] | | | 2.50 | BGO | 22 |

*4.4. Position reconstruction*

The lateral distribution of the electromagnetic shower allows a more accurate determination of the position of

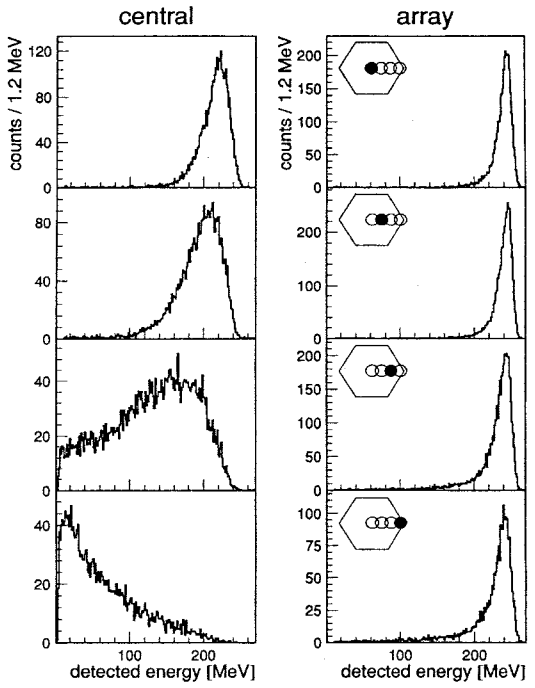


Fig. 13. The energy response as a function of impact point measured at an incident energy of $E_\gamma = 258$ MeV. The response of the central detector (left) and the total cluster (right) are shown in comparison to the central illumination.

impact of the photon than given by the granularity of the system. In general the impact point, $X$, can be obtained from a weighted average over the detectors that fired,

$$X = \frac{\sum_i w_i x_i}{\sum_i w_i}, \qquad (1)$$

where $x_i$ is the (two dimensional) position vector of the center of module $i$ and $w_i$ its relative weight. Two weighting procedures have been considered on the basis of GEANT3 simulations. Using linear weighting, $w_i = E_i$, results in a non-linear position reconstruction although. The true position can still be obtained from the relation $X = a \sinh(bX_{\text{true}})$, suggested by Baumeister et al. [15]. In the second approach proposed by Awes et al. [16] $w_i = \max\{0, [W + \ln(E_i/\Sigma_i E_i)]\}$ which for the TAPS configuration gives a linear dependence on position when $W = 5$. The latter procedure has been used in the present analysis.

The position resolution was studied experimentally by varying the point of incidence of the photon beam as shown in Fig. 5. The centroid position determined and the true location of the beamspot on the detector are compared in Fig. 14 for 300 MeV photon energy. The horizontal bars indicate the width ($\sigma$) of the beam spot, while the vertical bar represents the width of the reconstructed position distribution which is non-Gaussian (see below). The position response is found to be linear but the reconstructed positions do not coincide with the true values. The same analysis applied to simulated events (full circles), however, indicates the same linearity but reconstructs the true absolute position. The observed systematic displacement was found to increase with energy. It has been verified by GEANT3 that an incident beam direction not exactly normal to the front face of the detectors could have caused such a virtual displacement, which is energy dependent due to the increasing average depth of the shower. At 100 MeV photon energy the displacement amounts to about 1.2 mm/degree deviation from a perpendicular impact and increases to 2.6 mm/degree at 700 MeV. The observed difference between true and reconstructed positions is consistent, therefore, with the combined error of the absolute position (2 mm) and an orientation (2°) of the dectector block.

The position resolution depends strongly on the number of detectors which respond (cf. Fig. 8). When the cluster size is small the position distribution becomes non-Gaussian reflecting the hexagonal geometry. Indeed, at lower energies ($< 300$ MeV) the resolution is determined mostly by the granularity of the detector system. Only at higher energies the cluster size is large enough to determine a reliable centroid; here the resolution was found to be 19 mm (FWHM), after unfolding the spot size of the beam. More details on the position reconstruction can be found in ref. [10].

### 4.5. Analysis procedure

The experience gained in the operation of TAPS has resulted in an anlysis procedure which can be adapted to

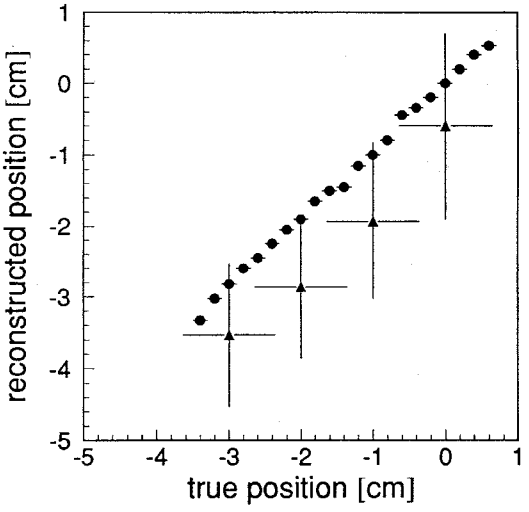


Fig. 14. Position reconstruction for the four beam positions indicated in Fig. 5. The incident energy was 300 MeV. GEANT3 results are given by full circles. See text for more details.

each specific experiment. For example, it is possible to maximize the acceptance of a block at the expense of resolution by allowing also detectors that are located on the edge of a block to serve as a central detector of a cluster. In view of the present results the GEANT3 simulations are then sufficient to determine whether the resolution (energy and position) is still acceptable for that experiment. Similar tuning can be made for the cluster size, which is important to discriminate multiple hits in a single block.

## 5. Summary

The response of the spectrometer TAPS to quasi-monochromatic photons in the energy range between 45 MeV and 790 MeV has been measured at the Mainz Microtron MAMI. The experimental performance has been described in detail and compared to Monte Carlo simulations based on the code GEANT3. When account is taken of light collection effects not included in the simulation, good agreement is obtained.

The energy resolutions achieved for the total light output and the fast scintillation component, respectively, reflect the excellent performance of the spectrometer and its unique capability to study neutral meson production in medium and high energy physics experiments with good sensitivity, resolution and particle discrimination capabilities.

The optimum method for the reconstruction of the point of impact has been investigated. The position of the primary photon has been determined from the logarithmically weighted center of gravity of the shower energy which spreads out over several detectors, but the angle of incidence of the photon must also be taken into account. The determination of the invariant mass as well as the deduced emission angle of the neutral meson benefits from a position resolution superior to the pure geometrical size of a single detector module.

## Acknowledgements

We would like to acknowledge the outstanding support of the accelerator people of MAMI, in particular K.H. Kaiser, as well as many other scientists and technicians of the Institut für Kernphysik at the University of Mainz during our stay at their institute. This work was supported by Deutsche Forschungsgemeinschaft (SFB 201), Bundesministerium für Forschung und Technologie (BMFT, contract No. 06 GI 174 I) and Gesellschaft für Schwerionenforschung (GSI, contract GI Met K). This work is also part of the research program of the Stichting voor Fundamenteel Onderzoek der Materie (FOM) with financial support of the Nederlandse Organisatie voor Wetenschappelijk onderzoek (NWO). The photon tagging facility was funded by the U.K. Science and Engineering Research Council.

## References

[1] R. Brun et al., GEANT3,CERN/DD/ee/84-1, (1986); W.R. Nelson, H. Hirayama and D.W.O. Rogers, EGS, SLAC-265 (1985).
[2] The TAPS collaboration: GSI (Darmstadt,Germany), GANIL (Caen, France), KVI (Groningen,The Netherlands), Universities of Giessen, Munich, Münster (Germany), University of Valencia (Spain).
[3] J. Ahrens et al., Proc. Int. Workshop on Future Detectors for Photonuclear Experiments, Edinburgh, May 1991.
[4] R. Novotny, IEEE Trans. Nucl. Sci. 38 (1991) 379.
[5] Phys. Rev. D, Particles and Fields 45 (1992), Review of Particle Properties, Part II.
[6] H. Beil and R. Bergere, CEA-N-2144, (1980).
[7] L. Cardman, Proc. Magnetic Spectrometer Workshop, Williamsburg, VA, Oct. 10–12, 1983.
[8] Th. Walcher, Prog. Part. Nucl. Phys. 24 (1990) 189.
[9] I. Anthony et al., Nucl. Instr. and Meth. A 301 (1991) 230.
[10] C. Molenaar, KVI internal report, (1992).
[11] T. Matulewicz et al., Nucl. Instr. and Meth. A 289 (1990) 194.
[12] A.R. Gabler, Diploma Thesis, University of Giessen, (1992), unpublished.
[13] N.N. Ershov et al., Opt. Spectrosc. USSR 53 (1982) 51; M. Laval et al., Nucl. Instr. and Meth. 206 (1983) 169.
[14] R. Novotny et al., Nucl. Instr. and Meth. A 262 (1987) 340.
[15] H. Baumeister et al., Nucl. Instr. and Meth. A 292 (1990) 81.
[16] T.C. Awes et al., Nucl. Instr. and Meth. A 311 (1992) 130.
[17] E. Bloom et al., Ann. Rev. Nucl. Part.Sci. 33 (1983) 143.
[18] B. Adeva et al., Nucl. Instr. and Meth. A 289 (1990) 35.
[19] C. Bebek, Nucl. Instr. and Meth. A 265 (1988) 258.
[20] E. Aker et al., Nucl. Instr. and Meth. A 321 (1992) 69.